Pergamon

Geochimica et Cosmochimica Acta, Vol. 62, No. 19/20, pp. 3285–3300, 1998

0016-7037/98 $19.00 + .00

PII S0016-7037(98)00222-1

Experimental and theoretical vibrational spectroscopic evaluation of arsenate coordination in aqueous solutions, solids, and at mineral-water interfaces

SATISH C. B. MYNENI,[1,*,†] SAMUEL J. TRAINA,[1] GLENN A. WAYCHUNAS,[2] and TERRY J. LOGAN[1]

[1]School of Natural Resources, Kottman Hall, The Ohio State University, Columbus, Ohio 43210, USA
[2]Earth Sciences Division, Lawrence Berkeley National Laboratory, Berkeley, California, 94720, USA

(*Received August* 20, 1997; *accepted in revised form June* 22, 1998)

Abstract—Arsenate (AsO_4^{3-}) is a common species in oxidizing aquatic systems and hydrothermal fluids, and its solubility and partitioning into different mineral phases are determined by the nature of AsO_4^{3-} coordination, solution pH, type of soluble cations, and H_2O structure at the mineral-fluid interfaces. While the vibrational spectroscopy has been widely used in examining the AsO_4^{3-} coordination chemistry, insufficient knowledge on the correlation of AsO_4^{3-} molecular structure and its vibrational spectra impeded the complete spectral interpretation. In this paper, we evaluated the vibrational spectroscopy of AsO_4^{3-} in solutions, crystals, and sorbed on mineral surfaces using theoretical (semiempirical, for aqueous species) and experimental studies, with emphasis on the protonation, hydration, and metal complexation influence on the As-O symmetric stretching vibrations. Theoretical predictions are in excellent agreement with the experimental studies and helped in the evaluation of vibrational modes of several arsenate-complexes and in the interpretation of experimental spectra. These vibrational spectroscopic studies (IR, Raman) suggest that the symmetry of AsO_4^{3-} polyhedron is strongly distorted, and its As-O vibrations are affected by protonation and the relative influence on AsO_4^{3-} structure decreases in the order: $H^+ \gg$ cation $\geq H_2O$. For all AsO_4^{3-} complexes, the As-OX symmetric stretching (X = metal, H^+, H_2O; $\leq$820 cm^{-1}) shifted to lower wavenumbers when compared to that of uncomplexed AsO_4^{3-}. In addition, the As-OH symmetric stretching of protonated arsenates in aqueous solutions shift to higher energies with increasing protonation ($<$720, $<$770, $<$790 cm^{-1} for $HAsO_4^{2-}$, $H_2AsO_4^-$, and $H_3AsO_4^0$, respectively). The protonated arsenates in crystalline solids show the same trend with little variation in As-OH symmetric stretching vibrations. Since metal complexation of protonated AsO_4^{3-} does not influence the As-OH vibrations significantly, deducing symmetry information from their vibrational spectra is difficult. However, for metal unprotonated-AsO_4^{3-} complexes, the shifts in As-OM (M = metal) vibrations are influenced only by the nature of complexing cation and the type of coordination, and hence the AsO_4^{3-} coordination environment can be interpreted directly from the splitting of As-O degenerate vibrations and relative shifts in the As-OM modes. This information is critical in evaluating the structure of AsO_4^{3-} sorption complexes at the solid-water interfaces. The vibrational spectra of other tetrahedral oxoanions are expected to be along similar lines. *Copyright © 1998 Elsevier Science Ltd*

1. INTRODUCTION

Arsenate (AsO_4^{3-}) is a predominant species of As in oxic waters, sediments, and hydrothermal fluids. With the exception of weathered profiles containing As sulfides (or As substituted pyrites), the low natural abundances of arsenate does not allow its formation as a pure mineral, and hence As commonly occurs as adsorbed species on sediment or soil minerals such as Fe- and Al-oxyhydroxides. Previous research has indicated that As is a labile element and that changing redox conditions, solution pH, and the presence of organic ligands in the environment modify the adsorbed arsenate speciation, solubility, and dispersion (Cherry et al., 1979; Cullen and Reimer, 1989; Masscheleyn et al., 1991). This suggests that knowledge on the coordination of soluble and adsorbed species is critical to the interpretation of speciation changes and their reaction rates with variations in the environmental conditions. Spectroscopic techniques such as X-ray absorption (Waychunas et al., 1993; Fendorf et al., 1997; Foster et al., 1998), low angle X-ray scattering (Waychunas et al., 1995), X-ray photoelectron (Soma et al., 1994), and vibrational spectroscopy (Harrison and Berkheiser, 1982; Lumsdon et al., 1984; Sun and Doner, 1996) have been applied to evaluate arsenate coordination in a variety of geologic materials. Of these, vibrational spectroscopy (both infrared and Raman) is particularly useful for the examination of in situ coordination of arsenate, specifically its protonation and solvation reactions, which other cited techniques lack. Since, the nature of protonation and solvation of adsorbed ions determines the strength of the sorption complexes and their chemical reactivity at the interfaces (Stumm, 1993), such in situ information is important in evaluating the As behavior in natural systems. Recent experimental studies on another species of As, arsenite (AsO_3^{3-}), in hydrothermal fluids have also indicated that its vibrational spectra contain a wealth of coordination information that can be interpreted accurately by comparison with theory (Pokrovski et al., 1996; Tossel, 1997). In this study we have evaluated arsenate speciation in aqueous solutions and different solid phases (adsorbed, structural As) using both theoretical and experimental methods. The analysis presented here is also useful for interpreting the coordination chemistry of other tetrahedral oxoanions.

The coordination chemistry of AsO_4^{3-} and other oxoanions

*Author to whom correspondence should be addressed (smyneni@lbl.gov).
†*Present address:* Mail Stop 90/1116, Earth Sciences Division, Lawrence Berkeley National Laboratory, Berkeley, California 94720, USA.

Table 1. Normal modes of AsO_4^{3-} in different symmetries.

	Normal Vibrations			
Symmetry	ν_1	ν_2	ν_3	ν_4
Td	A_1	E	F_2	F_2
C_{3v}	A_1	E	A_1+E	A_1+E
C_{2v}	A_1	$A_1 + A_2$	A_1+B_1+B_2	A_1+B_1+B_2
C_1	A	2A	3A	3A

have been studied with the help of vibrational spectroscopy for the last four decades, and a compilation of these studies has been published by Moenke (1962), Ross (1974), and Nakamoto (1986). For several compounds these studies listed the fundamental As-O vibrations without any reference to their AsO_4^{3-} structural environment. Hence little information is available to elucidate the overall structural and/or coordinating metal influences on As-O vibrations. Several of the recent studies were aimed at the IR of AsO_4^{3-} sorbed onto mineral surfaces, predominantly Fe-oxyhydroxide surfaces, and indicated that AsO_4^{3-} forms binuclear complexes by replacing surface OH^- (Harrison and Berkheiser, 1982; Lumsdon et al., 1984; Sun and Doner, 1996). These inferences were based on spectral interpretations, such as the splitting of As-O degenerate vibrational modes and the disappearance of peaks corresponding to particular types of OH^- functional groups (A, B, C types; Sposito, 1989). Unfortunately these studies do not distinguish the sorption of protonated and unprotonated AsO_4^{3-} and the relative influence of complexed Fe^{3+} and H^+ on As-O vibrations, and hence conclusions on AsO_4^{3-} coordination can not be made with certainty. The application of IR and Raman to the study of other AsO_4^{3-} containing systems is thus often limited due to insufficient structural interpretation. In this paper we have evaluated the structure and coordination chemistry of different AsO_4^{3-} complexes in solution and solids using their experimental vibrational spectra. We have also compiled the values available in the literature for AsO_4^{3-} vibrations in different minerals and reevaluated their assignments using the most recent crystal structure refinements. Additionally, theoretical vibrational spectra of simple AsO_4^{3-}-proton and -metal clusters were calculated. Together with experimental results on structurally known AsO_4^{3-} models, the calculations help provide a working hypothesis for the interpretation of spectral information in AsO_4^{3-} systems.

1.1. Symmetry and Vibrational Modes of AsO_4^{3-} Species

The Td symmetry of AsO_4^{3-} is rarely preserved in natural samples because of its strong affinity to protonate, hydrate, and complex with metals. Such chemical interactions reduce AsO_4^{3-} tetrahedral symmetry to either C_{3V}/C_3 (corner-sharing), C_{2v}/C_2 (edge-sharing, bidentate binuclear), or C_1/C_s (corner-sharing, edge-sharing, bidentate binuclear, multidentate). Changes in the vibrational spectra of AsO_4^{3-} associated with reduction in symmetry can be interpreted using group theory (Table 1; Cotton, 1971). In the infrared region, AsO_4^{3-} (or molecules in Td symmetry) exhibits nine normal modes, an A_1 (symmetric stretch, ν_1), an E (symmetric bending, ν_2), and two F (asymmetric stretching and bending, ν_3 and ν_4, respectively). The symbols A_1, E, and F correspond to nondegenerate and doubly and triply degenerate vibrations, respectively. In physical chemistry and spectroscopy literature both of these notations (A, E, F; ν_1, ν_2,. . .) are commonly used. Since the symbol 'ν' is used by several researchers to represent stretching vibrations only, it is possible to confuse some interpretations in the literature. For the reasons discussed later, our study focused at the stretching vibrations and we have chosen to use ν_s and ν_{as} for symmetric and asymmetric stretching. With these symbols we also specified the vibrating atom-pair to avoid any misinterpretations (e.g., ν_s of As-OH).

In association with AsO_4^{3-} symmetry and coordination changes, the A_1 band may shift to different wavenumbers, and the degenerate E and F modes may give rise to several new A_1, B_1, and/or E vibrations (Table 1). Very often the apparent structural symmetry of AsO_4^{3-} species in solutions, crystals, or in the vicinity of interfaces may not follow the above described symmetry predictions closely. Such discrepancies may be caused by: (1) extensive H-bonding of the non-bonding O atoms of AsO_4^{3-} with several H_2O molecules, (2) AsO_4^{3-} polydentate complexation with cations, and (3) tilt of AsO_4^{3-} complexed cation (or proton) away from the As-O-M (M = metal) axis (considered linear usually in symmetry analysis). For these reasons, the presence of high symmetry species in samples may not be excluded when their vibrational spectra exhibit all AsO_4^{3-} fundamental vibrations. Similarly, the appearance of single, unsplit peaks for degenerate As-O vibrations do not completely rule out the presence of low symmetry species in the samples. The symmetry of an AsO_4^{3-} group can be very low, in fact C_1, but not result in enough peak splitting to be identified. In summary, the disparity between the symmetry predictions and experimental data is due to the conservancy of finite spectral resolution and our commonsense perspective on symmetry. However, such deviations in apparent symmetry can be identified accurately with the chemical shift information from A_1 vibrational modes and the peak splittings of degenerate vibrations. Also for ions in crystals the applications of site symmetry and factor group analysis and correlation methods can offer more complete information on their vibrational spectra (Bhagavantam and Venkataraidu, 1969; Fateley et al., 1971). In this paper we show that energy shifts in A_1 vibrations, and the amount of splitting in degenerate vibrations are related to the strength of AsO_4^{3-} complexes.

2. DATA COLLECTION AND ANALYSIS

2.1. Theoretical Calculations

Semiempirical molecular orbital calculations were conducted using the PM3 method (for geometry optimization and vibrational spectra), which is based on the NDDO (Neglect of Diatomic Differential Overlap) approximation (Stewart, 1989a, b). Previous semiempirical calculations on smaller molecules have shown that PM3 produces results closer to the experimental values than to other available semiempirical methods (Stewart, 1989a,b; Seeger et al., 1991). PM3 considers overlap density between two orbitals centered on the same atom interacting with the overlap density between two orbitals also centered on a single atom. The result of neglecting correlated motion of the electrons and approximating the potentials as harmonic functions yields calculated vibrations usually at higher energies than the

experimental values. These computations were carried out with the Hyperchem computational chemistry software (Autodesk, Inc.).

The vibrational calculations were performed on molecules optimized geometrically (discussed later) and also on molecules constructed with bond lengths and angles obtained from published X-ray crystal structure refinement data. Although the predicted vibrational frequencies from these two methods do not differ greatly, the simulations performed on molecules with the literature bond lengths produced values closer to the experimental values for both ν_3 and ν_1 vibrations (<60 and <40 cm^{-1}, higher, respectively). Geometry optimization for the hypothetical molecules was conducted with a Restricted Hartree Fock (RHF) set up, and the termination condition was set with Polak and Ribiere approximation. The convergence limit was usually $\sim$0.01 kcal (mol Å)$^{-1}$. The bond lengths and angles of geometrically optimized molecules (e.g., AsO_4^{3-}, $HAsO_4^{3-}$,) are in good agreement with the experimental values (from EXAFS measurements, Myneni, 1995). Since the bond parameters are not available for particular arsenate complexes of interest in this study (e.g., certain metal arsenates), geometry optimized arsenate species were used to compute vibrational spectra. The calculations include partially and fully solvated AsO_4^{3-}, $HAsO_4^{3-}$, $H_2AsO_4^-$, and $H_3AsO_4^0$ molecules, which represent AsO_4^{3-} in different solvation states within minerals or on their surfaces (e.g., Fig. 1). The effect of a complexing metal on As-O vibrations was studied by selecting solvated bidentate mononuclear metal AsO_4^{3-} (edge-sharing) complexes as models. In this study, Al-, Mg-, Cd- and Zn-AsO_4^{3-} complexes were examined since only these metals were parameterized in PM3. Single molecule clusters with a maximum number of eighteen atoms were used in the calculations (e.g., solvated $HAsO_4(H_2O)_4^{2-}$). In the case of cationic complexes, the complete coordination shell of the cations was not included because of size limitations of the cluster. The molecular orbital calculations exaggerate the effect of species on the outside of the cluster, and hence the exclusion of all ligands in the coordination environment of cations (type of attached ligand, and coordination number) can change the As-O vibrations. This effect may be pronounced for high charged species, such as Al^{3+} and Fe^{3+}. Overall the magnitude of this effect is smaller than the direct cation-arsenate interactions. Since the semiempirical methods use the parameters obtained from the experimental data, and the computed force constants have been scaled to fit the experimental data, even the smaller clusters can produce reasonably agreeable results. Although larger atomic clusters predict the experimental data more accurately, such a level of complexity was beyond the computational resources available. These features do not limit the overall interpretation of results in this study. This is because: (1) the predicted As-O bond lengths and the vibrational frequencies are close to the experimental values and (2) the theoretically obtained information was used mainly to examine and to explain the trends in vibrational frequencies rather than to predict the actual bond lengths and vibrational frequencies.

2.2. Infrared Spectroscopy

Fourier Transform infrared spectra (FTIR) of AsO_4^{3-} containing samples were examined on a Mattson Polaris FTIR spectrometer equipped with a broad-band, N_2 cooled mercury-cadmium-telluride (MCT) detector and a KCl beam splitter. The sample scans ranged from 4000 to 400 cm^{-1} with 1 cm^{-1} resolution and were collected as an average of 200 scans. Diffuse reflectance FTIR spectra of solid samples were collected with the help of a Harrick Praying-Mantis diffuse reflectance cell. For spectral collection, all solid samples were powdered and diluted with IR-grade KBr (2% sample). Background subtractions were made for the diluent.

Aqueous arsenate and other oxoanion containing samples were examined using an attenuated total reflectance (ATR) cell with a premounted ZnSe reflection crystal (size: 8 × 8 × 33 mm, 9 reflections). To minimize oxoanion reactions with the ZnSe crystal, the spectra were collected immediately after the solutions were transferred into the ATR cell. However, the spectra were invariant from $<$0.017–1 h. Background subtractions were made to remove the bulk water spectra.

2.3. Raman Spectroscopy

Raman laser excitation was provided by a Ti: sapphire laser (Coherent) pumped by an Ar laser (Coherent 90) operating at 784 nm and filtered by a holographic band pass filter (Kaiser) which delivered about 50 mW near the sample. A single stage spectrograph (Instruments SA, HR 640) with a 300 mm^{-1} grating coupled to a CCD detector (photometric CH260 camera head/EEV05-10CCD with 296 × 1152 pixels, 0.66 cm × 2.59 cm active area) in 180° backscattering geometry was used to detect the signal from the sample. A holographic band reject filter (Kaiser) was also used in front of the CCD detector. The scans were collected from 2000 to 200 cm^{-1} with a step size of 1.5 cm^{-1}. Depending on the solid phase sorbate concentration and background fluorescence, the scan time ranged from less than a minute to a maximum of 15 min. The scans were collected at low energy laser output to avoid local heating in the sample.

2.4. Sample Preparation

Aqueous spectra of arsenate and other oxoanions were examined by dissolving their Na salts in deionized water. Of these salts, only protonated oxoanion containing Na salts were used for preparing As and P containing solutions (10 mM). When required, pH of these solutions was adjusted by adding NaOH, HCl, H_2SO_4, and HNO_3. Arsenate adsorption on portlandite was conducted at the equilibrium pH of portlandite (pH $\sim$12.6). Adsorption experiments were conducted for portlandite by reacting 0.1 g of reagent grade CaO with As-containing solutions (0–3.6 mM). Adsorption onto reagent grade gibbsite was also conducted under the same conditions, but at the equilibrium pH of gibbsite (pH: 6.5–8.2). The sorption procedures and their mass balance results were described in detail by Myneni, 1995. Sample preparation procedures for As-reacted ettringite and a detailed description of their vibrational spectra are described by Myneni et al., 1997; and Myneni et al., 1998, respectively. Crystalline arsenate salts of different cations were obtained from Smithsonian Museum and from the mineral collection of the Department of Geological Sciences at The Ohio State University. A sample of aluminum arsenate (poorly crystalline, with several molecules of crystalline water) was obtained from B. Rochette and S. Fendorf of the University of Idaho (pers. commun.).

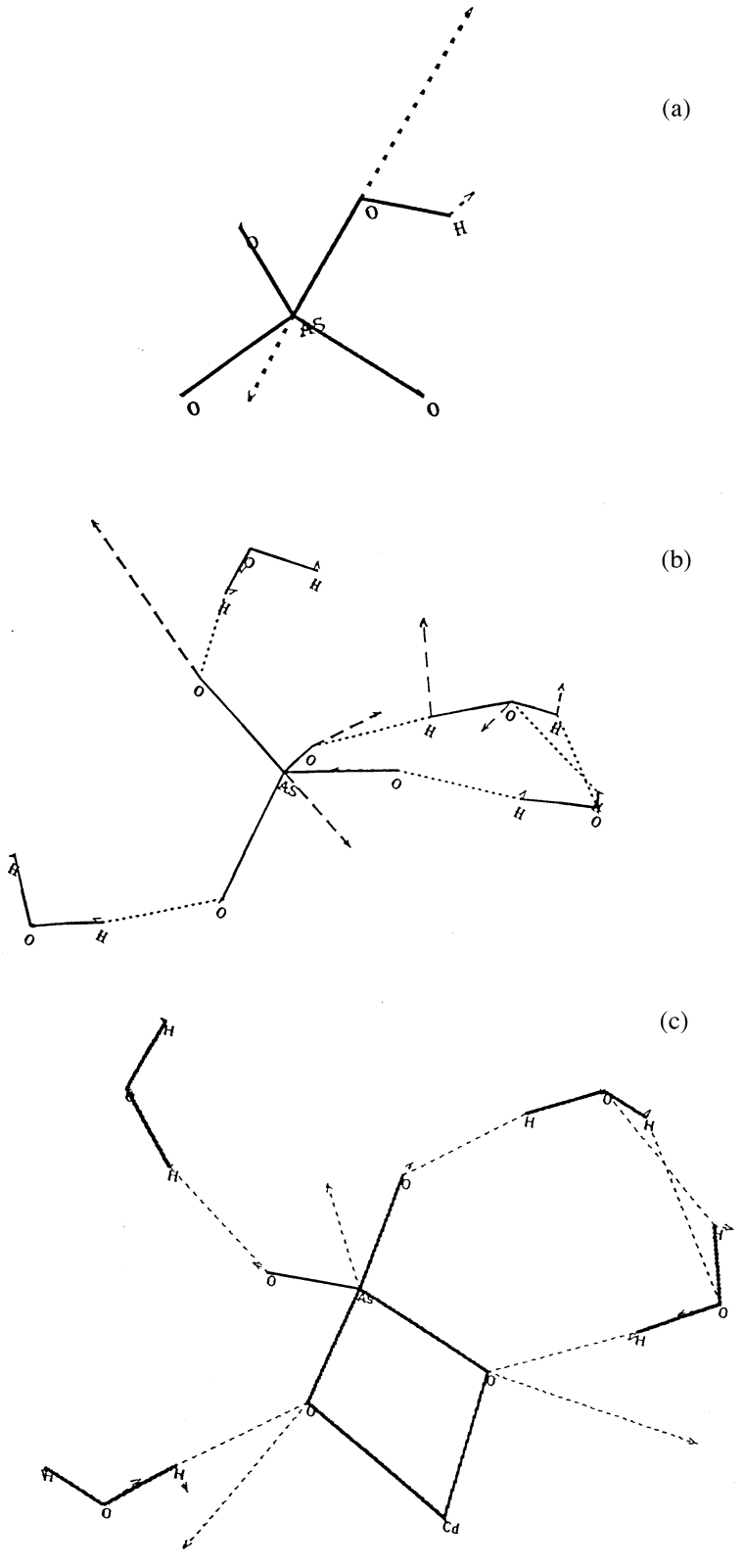

Fig. 1. Examples of AsO_4^{3-} molecular clusters used for theoretical vibrational spectra calculations. Solid and dashed lines correspond to interatomic and H-bonds, respectively. Long dashed lines with arrow heads represent symmetric stretching vibrations. The structures are for protonated (a), solvated (b), and metal complexed AsO_4^{3-} (c).

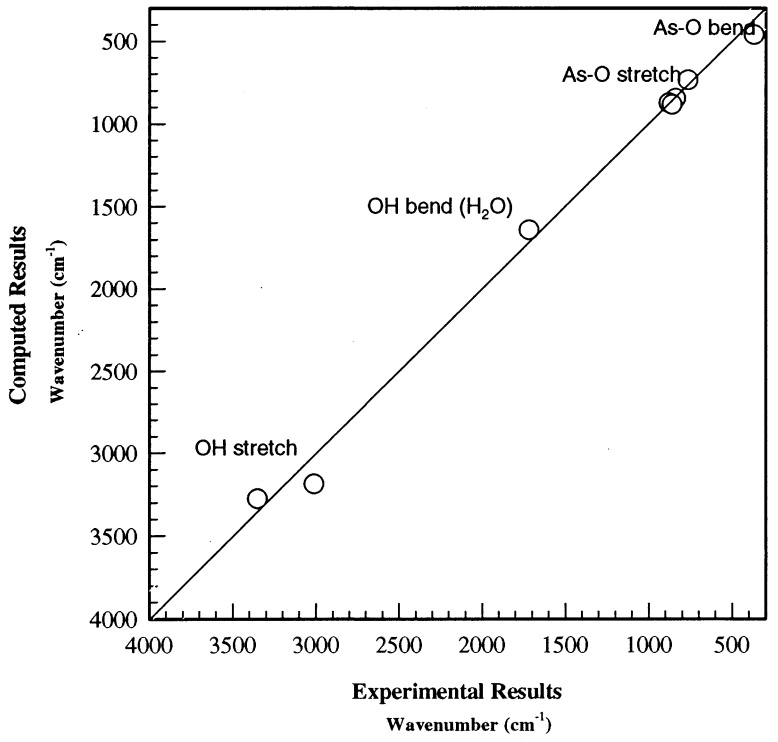

Fig. 2. Comparison of theoretical and experimental vibrational spectra of different AsO_4^{3-} species. Refer Table 2 for further details. The points around 3000, 1600, 800, and 400 cm^{-1} correspond to the OH stretching, OH bending, As-O stretching, and As-O bending vibrations, respectively.

2.5. Spectral Deconvolution and Analysis Procedures

The collected FTIR and Raman spectra were processed for peak deconvolution and curve fitting with the Grams 3.02 software package (Galactic Industries Corp.). When superimposed peaks were noticed (from the peak asymmetry and appearance of shoulders), second-order derivatives were used to identify the number of overlapping peaks and their approximate peak positions, and curve fitting was later employed to obtain information on peak intensities and positions. The composite peaks were fit with Cauchy-Lorentzian profiles, using nonlinear least squares refinement procedures based on a finite difference Levenberg-Marquardt algorithm (Maddams, 1980; Gillette et al. 1982). The peak positions obtained from direct curve fitting and peak second derivatives were close and differed by less than 10 cm^{-1} in all samples. However, when peaks did not overlap, their positions were identified with more accuracy ($\pm$2.0 cm^{-1}).

3. RESULTS AND DISCUSSION

Vibrational spectra of AsO_4^{3-} containing solids and solutions exhibit (1) As-O vibrations and (2) OH and H-bond vibrations from solvated H_2O (As-O$\cdots H_2O$; '$\cdots$' represents H-bond, see Fig. 1). The group frequencies of AsO_4^{3-} and H_2O are useful to interpret the nature of AsO_4^{3-} interactions and coordination chemistry. While As-O vibrations of AsO_4^{3-} in Td symmetry occur at 818 (A_1), 786 (F-stretching), 405 (F-bending), and 350 cm^{-1} (E), (Vasant et al., 1973), the O-H vibrations of liquid H_2O occur at 3615 (B_1), 3450 (A_1), and 1640 (B_2) cm^{-1} (Nakamoto, 1986). The $O_{oxoanion}\cdots H_{H2O}$ (H-bond) vibrations were not studied because of their low intensity and occurrence in the far-IR region ($\sim$300 cm^{-1}; Brooker, 1986; Brooker and Tremaine, 1992). In this study, we focused on the stretching vibrations since these can be interpreted and correlated easily with changes in coordination environment. Also, the stretching vibrations occur at higher energies than those of bending and so can be distinguished clearly from the rotational modes of the molecules and the lattice vibrations of the crystal.

3.1. Theoretical Calculations on Aqueous AsO_4^{3-} and its Complexes

PM3 based semiempirical calculations were performed to examine the variation in As-O ν_s and ν_{as} vibrations with AsO_4^{3-} solvation, protonation, and metal complexation. The calculated ν_s and ν_{as} (or its degenerate mode) AsO_4^{3-} vibrations are higher than the experimental values of aqueous species, but the differences are within 35 and 100 cm^{-1}, respectively (Fig. 2). These minor differences are mainly due to the assumptions involved in the calculations and to the difference between gas phase vs. condensed phase intermolecular interactions. The OH_{H2O} vibrations (OH vibrations of H_2O molecule; this notation is used in this paper to distinguish the OH vibrations of As-OH and H_2O molecules) obtained from these calculations poorly represent AsO_4^{3-} solvation and deviate from the experimental values (Fig. 2). This is because the anion solvated first-shell H_2O molecules form H-bonds with outer solvated molecules in aqueous solutions (or other cations in solids) and accounts for $<$60% of the total solvation energy (Markham et

Table 2. Theoretical bond lengths and stretching vibrations for different AsO_4^{3-} species.

Molecule	Bond Length (Å)		Stretching Vibrations (cm^{-1})			
	As-OX (X = H^+, cation, H_2O)	As-O	As-OX (X = H^+, cation, H_2O)		As-O	
			ν_s	ν_{as}	ν_s	ν_{as}
AsO_4^{3-} (g)	--	1.74	ν_s: 773, ν_{as}: 824			
$HAsO_4^{2-}$(g)	1.88	1.68	637		823	905
$H_2AsO_4^-$(g)	1.81	1.64	744	733	880	957
Solvated AsO_4^{3-}						
$AsO_4^{3-}(H_2O)$	1.76	1.73	806		844	946
$AsO_4^{3-}(H_2O)_2$	1.75	1.72	836	821	863	923
$AsO_4^{3-}(H_2O)_4$	---	1.73	ν_s: 849, ν_{as}: 878			
Protonated Aq. AsO_4^{3-}						
$HAsO_4^{2-}(H_2O)_4$†	1.87	1.68	684	697	895	944
$H_2AsO_4^-(H_2O)_4$	1.81	1.63	781	758	937	1041
$H_3AsO_4^0(H_2O)_4$	1.76	1.60	805	812	998	
Metal Complexed Aq. AsO_4^{3-}						
Al-O_2-$AsO_2(H_2O)_4$	1.88	1.62	637	637	1008	1037
Mg-O_2-$AsO_2(H_2O)_4$	1.80	1.65	794	696 (?)	925	986
Cd-O_2-$AsO_2(H_2O)_4$	1.79	1.66	754	826	910	976
Zn-O_2-$AsO_2(H_2O)_4$	1.79	1.64	756	799	928	1004

† The symmetry of $HAsO_4^{2-}(H_2O)_4$ is not C_{3v}. See text for discussion.

al., 1996). In solids H_2O molecules bond to cations and also form H-bonds with AsO_4^{3-} simultaneously, and hence these H_2O molecules are chemically different from the AsO_4^{3-} solvated H_2O used in the calculations.

Theoretical calculations indicate that protonation, metal complexation, and H_2O H-bonding of AsO_4^{3-} results in increased As-OX (X = H^+, metal, or H_2O) bond length relative to the uncomplexed As-O (Table 2). Excepting for Al-AsO_4^{3-} complexes, protonation caused greater changes in the As-O bond length when compared to metal complexation and H-bonding. On the whole, the As-OH and As-O bond distances in polyprotic AsO_4^{3-} decrease in the order $HAsO_4^{2-} > H_2AsO_4^- > H_3AsO_4^0$, and with similar patterns for H-bonded As-O bonds [AsO_4^{3-} $(H_2O) > AsO_4^{3-}$ $(H_2O)_2$]. It should also be noted that the OH bond in $HAsO_4^{2-}$ bends towards one of its other uncomplexed oxygen atoms (Fig. 1a). This produces unequal $As\text{-}O_{uncomplexed}$ bond distances, and the symmetry deviates from C_{3v}, which would ordinarily predicted by group theory. However, as discussed earlier, the sample vibrational spectra can provide information on such symmetry deviations. Theoretical studies also indicate that the As-O bond distances of solvated AsO_4^{3-} are 1.73 Å and are shorter than the As-O distances in unsolvated species (1.74 Å). The same behavior was also observed in the case of experimentally verified protonated sulfates, e.g., in the case of S-OH bond lengths of gaseous (1.57 Å) and solvated (1.53 Å) H_2SO_4 species (Moodenbaugh et al., 1983).

The model calculations indicate a strong inverse relation between the As-O bond length and the shifts in ν_s vibrations (Table 2). For protonated and hydrated AsO_4^{3-}, the increases in As-OX bond length caused the ν_s of As-OX to decrease in the order AsO_4^{3-} $(H_2O)_2 > AsO_4^{3-}$ $(H_2O) \sim H_3AsO_4^0(H_2O)_4 > H_2AsO_4^-$ $(H_2O)_4 > HAsO_4^{2-}$ $(H_2O)_4$. These trends indicate that addition of a proton to AsO_4^{3-} strongly disturbs the As-O bond lengths. Addition of another proton to $HAsO_4^{2-}$ diminishes the influence of the first proton, and consequently the two As-OH bond lengths in $H_2AsO_4^-$ are shorter than that of As-OH in $HAsO_4^{2-}$. Such complexation reactions with some oxygen atoms of AsO_4^{3-} cause an increase in the bond order of uncomplexed As-O bonds, and in turn their As-O bond distances decrease (Table 2). This produces a blue shift in the ν_s of $As\text{-}O_{uncomplexed}$ vibrations, which increase in the order AsO_4^{3-} $(H_2O) < AsO_4^{3-}$ $(H_2O)_2 < HAsO_4^{2-}(H_2O)_4 < H_2AsO_4^-(H_2O)_4 < H_3AsO_4^0(H_2O)_4$. This general feature has also been observed in experimentally obtained bond lengths and vibrational frequencies of several other oxoanions, such as PO_4^{3-}, SO_4^{2-}, MoO_4^{2-}, and VO_4^{3-} (Cruickshank and Robinson, 1966; Payen

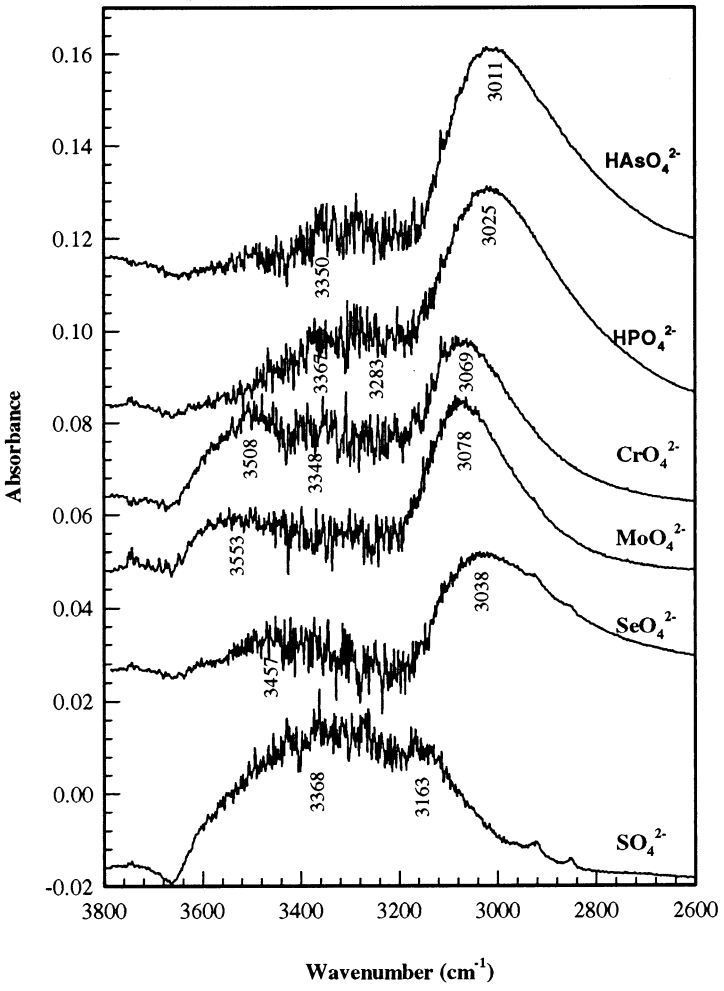

Fig. 3. ATR-FTIR spectra of OH stretching vibrations of H_2O in the primary oxoanion solvation shell. Oxoanion concentration in aqueous solutions was 10 mM, and the samples were prepared by dissolving Na-salts. Predominant aqueous species of oxoanions are shown with their respective spectra.

at al., 1987; Twu and Dutta, 1989; Persson et al., 1996). For metal arsenates, the As-OX bond distances and related ν_s vibrations vary with the type of complexed metal atom and its inductive effects on AsO_4^{3-} polyhedra. Of all the examined metals Al was the most effective in distorting the AsO_4^{3-} tetrahedron. Accordingly, the ν_s of As-OX vibrations shifted to 637 cm^{-1} for Al as compared to 794, 756, and 754 cm^{-1} in the case of Mg, Zn, and Cd, respectively. Although ν_{as} vibrations showed similar trends as those of ν_s, they are not very distinct (Table 2).

In summary, the calculated As-O vibrational modes agree with measured experimental values (Vasant et al., 1973; Farmer, 1974; Myneni, 1995), and the following conclusions can be drawn from theoretical calculations: (1) the AsO_4^{3-} tetrahedron is distorted more by protonation than by solvation, (2) with the exception of Al-AsO_4^{3-}, the ν_s bands of As-OH (as in $HAsO_4^{2-}$), As-$(OH)_2$ (as in $H_2AsO_4^-$), As-$(OH)_3$ (as in $H_3AsO_4^0$), and As-OM (M = complexing cation) of AsO_4^{3-} complexes shifted to <700, <780, <805, and $750-830$ cm^{-1}, respectively. Al produced a strong shift in the ν_1 band (637 cm^{-1}), which may have been due to the differences in electronegativity and charge.

3.2. Experimental Studies on AsO_4^{3-} Species

3.2.1. Structure of AsO_4^{3-}-solvated H_2O

To examine the nature of solvated water around AsO_4^{3-}, ATR-FTIR experiments of aqueous AsO_4^{3-} (10 mM) were conducted by subtracting the bulk water contributions using deionized water as a blank. Such subtraction procedures are valid since the structure and the intermolecular forces of the bulk water in AsO_4^{3-} aqueous solutions are the same as those in the deionized water (Brooker, 1986; Krestov et al., 1994). The charge contribution from aqueous ions diminish exponentially away from the ion, and after a few shells of solvated H_2O, the outer H_2O molecules behave as bulk water (Magini et al., 1988; Ohtaki and Radnai, 1993). The OH vibrations of $HAsO_4^{2-}$-solvated water are also compared with those of other oxoanions, such as HPO_4^{2-}, SO_4^{2-}, CrO_4^{2-}, SeO_4^{2-}, and MoO_4^{2-} (10 mM solutions, Fig. 3). Since Na-salts were used as the source of oxoanions, the OH vibrations correspond to the solvation of both Na^+ and oxoanions. However, previous studies using X-ray scattering techniques have shown that the oxoanion has

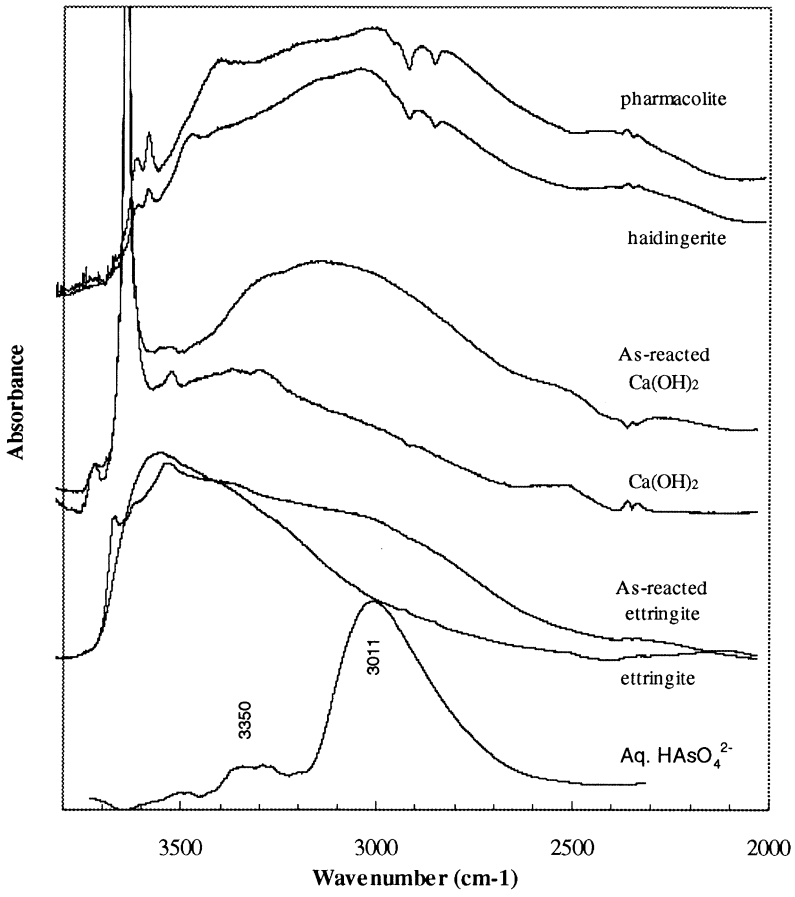

Fig. 4. OH stretching vibrations of structural H_2O in hydrated arsenate salts. All the spectra were collected using diffuse reflectance set up.

a greater influence on the structure of ion solvated water than Na^+ ions (Magini, et al., 1988; Ohtaki and Radnai, 1993).

The results indicate that H_2O in the oxoanion solvation shell exhibits strong OH stretching and bending vibrations at wavenumbers > 3000 cm^{-1} and around 1640 cm^{-1}, respectively. The smaller peaks at wavenumbers > 3200 cm^{-1} correspond to the OH ν_s and ν_{as} vibrations of H_2O in outer-oxoanion solvation (second and higher) shell and OH ν_{as} vibrations of inner-shell H_2O (Fig. 3). Since Na^+ coordinated H_2O also produce IR bands in the same region, it is difficult to separate their individual contribution. The oxoanion ATR-FTIR spectroscopic data indicate that different oxoanions exhibit OH vibrations at different energies (Fig. 3) and deviate from those of bulk H_2O, which occur at 3615, 3450, and 1640 cm^{-1} for ν_{as}, ν_s, and bending OH modes, respectively (Nakamoto, 1986). The observed relative chemical shifts of OH stretching vibrations of H_2O in oxoanion primary solvation shell correspond to the differences in the strength of H-bonding between the oxoanions and H_2O (Fig. 3). The oxoanions with strongest H-bonding with H_2O exhibit weaker OH stretching vibrations and consequently shift to lower wavenumbers. Inverse relation between the bond lengths of H-bond and OH and associated correlation with their respective vibrations and bond valence parameter have been reported previously for hydrated salts (Nakamoto et al., 1955; Brown and Altermatt, 1985; Barger et al., 1997). The strongly hydrating oxoanions also have high pKa values and narrower M-O vibrational bands. For example, CrO_4^{2-} and $HAsO_4^{2-}$, have OH stretching at 3069, and 3011 cm^{-1}, and their final pK_a (dissociation of $HCrO_4^{2-}$, $HAsO_4^{2-}$) are at 6.51 and 11.49, respectively (Fig. 3; Dove and Rimstidt, 1985; Brookins, 1988). Such spectral features were also reported for other anions using shifts in OD vibrations (for anions in HDO) and the narrowing of M-O vibrations (Bergström et al., 1991; Brooker and Tremaine, 1992). The details are not pertinent here, and their discussion will be presented in our future publication. These data confirm that the OH stretching vibrations of structural H_2O in crystals and aqueous solutions exhibit features characteristic of particular oxoanions. On the whole, the OH bending vibrations at $\sim$1640 cm^{-1} show the same features as those of stretching vibrations, but the spectral shifts are small and indistinct.

The vibrational spectra of crystalline hydrated arsenate salts with H-bonding between AsO_4^{3-} and H_2O exhibit OH vibrations similar to those described above (Fig. 4). The X-ray crystal structure refinement data for sodium arsenate ($Na_2HAsO_4 \cdot 7H_2O$), haindingerite ($CaHAsO_4 \cdot 2H_2O$), pharmacolite ($CaHAsO_4 \cdot 2H_2O$), and sainfeldite ($Ca_5(HAsO_4)_2\,(AsO_4)_2 \cdot 4H_2O$) indicate that the AsO_4^{3-} polyhedra form H-bonds with H_2O (Ferraris, 1969;

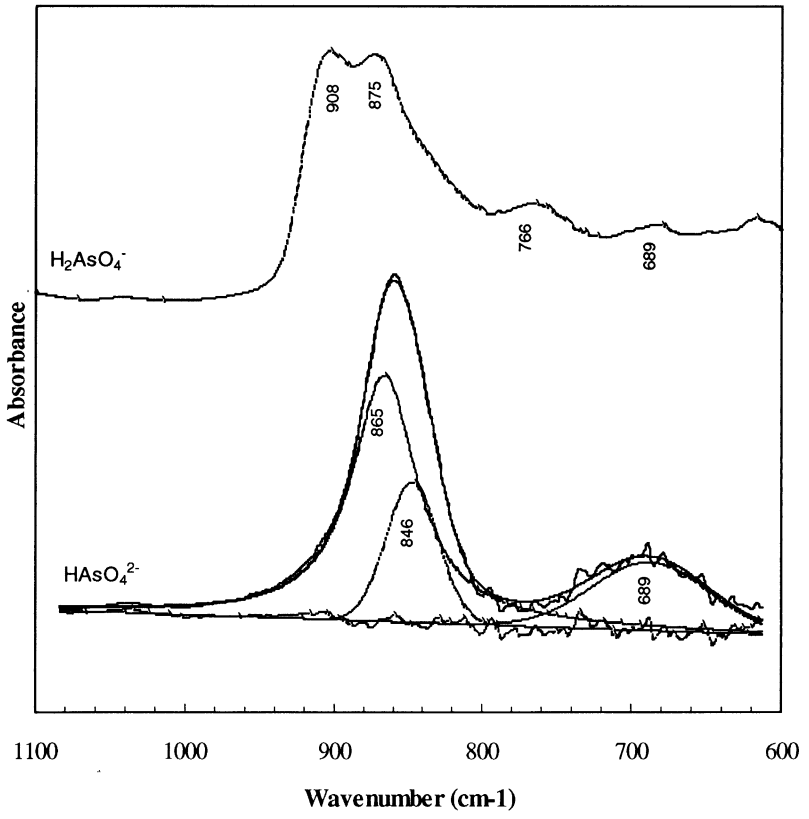

Fig. 5. ATR-FTIR spectra of As-O stretching vibrations of $HAsO_4^{2-}$ and $H_2AsO_4^-$. For spectral assignments refer Table 3.

Baur and Khan, 1970; Ferraris et al., 1972; Ferraris and Abbona 1972). Consequently their vibrational spectra indicate a strong IR absorption band around 3000 cm^{-1} corresponding to OH vibrations (Fig. 4). This feature is also evident in the IR spectra of ettringite, portlandite, and schwertmannite (Myneni, 1995; Carlson et al., 1998) in which the OH band shifts nearer to 3000 cm^{-1} upon their reaction with AsO_4^{3-}. The strong IR absorbance band around 3000 cm^{-1} in all of these solids is similar to that of solvated AsO_4^{3-} in aqueous solutions and corresponds to H-bonding between AsO_4^{3-} and the structural H_2O. Similar spectral features are expected when AsO_4^{3-} complexes on mineral surfaces and forms H-bonds with mineral-surface hydroxyls and/or adsorbed water.

3.2.2. Protonation influence on AsO_4^{3-} vibrations

AsO_4^{3-} is the dominant arsenate species in hyper-alkaline solutions and protonates to form $HAsO_4^{2-}$ and $H_2AsO_4^-$ around neutral pH and to form $H_3AsO_4^0$ in acidic pH ($H_3AsO_4^0$, pK_a = 2.24, 6.86, 11.49; Dove and Rimstidt, 1985). The symmetries of these four aqueous species with increasing proton concentration are Td, C_{3v}, C_{2v}, and C_{3v}. In the absence of symmetry deviations, $HAsO_4^{2-}$, in C_{3v} symmetry exhibits a ν_s As-OH (As-O for $H_3AsO_4^0$), and ν_{as} and ν_s As-O_3 [As-$(OH)_3$ for $H_3AsO_4^0$] vibrations. Similarly $H_2AsO_4^-$ (C_{2v}) should exhibit As-OH and As-O ν_{as} and ν_s vibrations.

The ATR-FTIR spectra of aqueous solutions of $HAsO_4^{2-}$, (pH = 9.1) exhibit a single As-O stretching peak at 859 cm^{-1} (peak width at half height = 57 cm^{-1}), which also tails to higher wavenumbers (Fig. 5). Curve fitting of this peak with two components produced peaks at 865 and 846 cm^{-1} which correspond to the ν_{as} and ν_s As-$O_{uncomplexed}$ vibrations, respectively (Fig. 5). In addition, the ATR-FTIR spectra of $HAsO_4^{2-}$ show a broad peak for ν_s of As-OH around 680-700 cm^{-1}. These values and the band assignments are in agreement with those of previous Raman studies (Table 3; Vasant et al., 1973).

Aqueous solutions of $H_2AsO_4^-$ (pH = 5.7) showed distinct As-$O_{uncomplexed}$ bands at 908 (ν_{as}) and 877 (ν_s) cm^{-1} and a broad band at ~766 cm^{-1} consisting of ν_{as} + ν_s of As-$(OH)_2$ modes (Fig. 5, Table 3). These spectral features agree with group theory predictions of a C_{2v} molecule. In addition, a shoulder at 847 cm^{-1} and a small peak at 689 cm^{-1} represent the As-O and As-OH vibrations of $HAsO_4^{2-}$ species in the sample. Since the pH of these samples was closer to the second pKa of arsenic acid (6.86 and ~6.5 at ionic strength = 0.2 mol_c L^{-1}), the presence of both $H_2AsO_4^-$ and $HAsO_4^{2-}$ are expected in the examined aqueous solutions.

The ATR-FTIR spectra of $H_3AsO_4^0$ and AsO_4^{3-} species could not be examined because of the instability of ZnSe ATR crystal in extremely low and high pH solutions. While previous Raman studies on $H_3AsO_4^0$ indicate that the As-$(OH)_3$ and As-O ν_s bands appear at 769 cm^{-1} and 923 cm^{-1}, respectively (Vasant et al., 1973), several numbers are reported for ν_{as} and ν_s of AsO_4^{3-} (Siebert, 1966; Müller and Krebs, 1967; Vasant et al.,

Table 3. **As-O vibrations of aqueous AsO_4^{3-} and protonated-AsO_4^{3-}**

Species (symmetry)†	As-O Stretching Vibrations (cm^{-1})			
	As-OH		As-O (uncomplexed)	
	ν_{as}	ν_s	ν_{as}	ν_s
AsO_4^{3-} (Td)	837 (ν_s), 878 (ν_{as})[a] 810 (ν_s), 810 (ν_{as})[b] 818_R (ν_s), 791_R (ν_{as})[c] 814_R (ν_s), 794_R (ν_{as})[d]			
$HAsO_4^{2-}$ (C_{3v}) (pH = 9.1)	680-700_{IR}[e]		865_{IR}[e]	846_{IR}[e]
(Ref., e: Na-salt, c: K-salt)	707_R[c]		866_R[c]	838_R[c]
$H_2AsO_4^-$ (C_{2v}) (pH = 5.7)	$\nu_s+\nu_{as}$: 759-766_{IR} (broad)[e]		908_{IR}[e]	875_{IR}[e]
(both references used Na-salts)	765_R[c]	745_R[c]	915_R[c]	875_R[c]
TlH_2AsO_4[f] (solution), (C_{2v})	760_R	742_R	913_R	876_R
$H_3AsO_4^0$ (C_{3v})	808 (E)$_R$[c]	769_R[c]	ν_s: 923_R[c]	

Subscripts R, and IR indicate that the data is collected using Raman, IR spectrometers. Superscripts represent the references for spectroscopic information. a) Nakamoto (1986), b) Siebert (1966) and Müller and Krebs (1967), c) Vasant et al. (1973), d) Eysel and Wagner (1993), e) this study, and f) Ouafik et al. (1995), Ouafik et al. (1996).

† AsO_4^{3-} symmetry is given in parenthesis.

1973; Nakamoto, 1986; Eysel and Wagner, 1993). Excepting those reported by Nakamoto (1986), all other literature values are closer to those reported by Vasant et al. (1973). Nakamoto (1986) incorrectly quoted the As-O vibrations reported by Siebert (1954).

In summary, the ATR-FTIR spectra of protonated arsenates and their band assignments are in excellent agreement with the previous Raman studies (Table 3). These studies indicate that (1) As-OH, As-$(OH)_2$, and As-$(OH)_3$ ν_s shifts to lower wavenumbers than the uncomplexed As-O ν_s vibrations and (2) As-OH ν_s of polyprotic AsO_4^{3-} increases in the order As-OH < As-$(OH)_2$ ≤ As-$(OH)_3$, with increasing proton concentration on AsO_4^{3-} molecule. These observations are also in agreement with those made from theoretical calculations.

The IR spectroscopic examination of solid phases containing protonated AsO_4^{3-} indicate that their As-O group frequencies are similar to those reported for aqueous spectra (Table 4). The crystal structure refinements of Na- and Ca-protonated arsenates indicate that the As-OH bond length is much longer than those of the unprotonated, metal complexed, and H-bonded As-O pairs (Ferraris, 1969; Baur and Khan, 1970; Ferraris et al., 1972; Ferraris and Abbona 1972). Since the bond valence at the protonated O atoms of AsO_4^{3-} polyhedra is already balanced (As-O = 1.25 v.u., O-H ~ 0.73 v.u.), these O atoms do not form any additional bonds with other structural atoms. Consequently, the As-OH bond length is manifested only by the nature of bonding at the remaining unprotonated O atoms of the arsenate polyhedra, and the intensity of H-bonds with the H^+ of As-OH. As predicted from theoretical calculations and also discussed later, the metal atoms are not as strong as H^+ in perturbing the As-OH bonds in protonated arsenate. For this reason, the As-OH and As-O vibrational modes of $HAsO_4^{2-}$ and $H_2AsO_4^-$ are very similar in solids and in aqueous solutions (Tables 3 and 4).

3.2.3. Metal complexation influence on AsO_4^{3-} vibrations

The vibrational spectra of metal arsenate complexes are more complex and difficult to interpret than those of protonated arsenates. Metal arsenate complexes in aqueous solutions exhibit shifts in As-OM (M = metal) ν_s vibrations and the degenerate modes split according to the type of interactions, such as ion-pair, monodentate complex, bidentate complex, and/or polymer formation. For different metal-arsenate complexes in the same geometry, shifts in ν_s vibrations represent variation in metal-arsenate bond strength and hence are characteristic of the metal atom. In metal arsenate solids polydentate complexes are common, and the As-O vibrational modes are difficult to interpret using the AsO_4^{3-} molecule group frequencies. In such cases, the normal modes of each As-O bond can be explained using an AsOM (M = metal) atom cluster (Nakamoto, 1986). Even with such analysis, spectral resolution limits the identification of each type of As-OM vibrations. As discussed later, metal complexation of protonated arsenates can be studied with the help of AsO_4^{3-} group frequencies. However, identification of molecule symmetry has to be evaluated with caution for all these cases. In this study we focused at the As-OM and As-$O_{uncomplexed}$ ν_s vibrations to describe the strength of the metal-arsenate complexes.

Metal complexation with AsO_4^{3-}. The vibrational spectra of examined Ca, Mn, Fe, Co, Ni, Cu, and Zn AsO_4^{3-} complexes in crystalline hydrated solids indicate that the As-OM ν_s vibrations shifted to different energies when compared to the aqueous AsO_4^{3-} (Table 4, Figs. 6–8). For example, the transition metal arsenates, such as those of Mn, Fe, Co, Ni, Cu, and Zn exhibit a red shift for ν_s vibrations to 780, 806, 794, 804, 790, and 790 cm^{-1}, respectively (Table 4, Moenke, 1966). The vibrational spectra of Al-arsenate, as predicted by theoretical studies, showed a strong shift for As-OAl vibrations (740 cm^{-1}). While these shifts are specific to the type of complexed

Table 4. **As-O vibrations of metal AsO_4^{3-} complexes in crystals.**

Species (symmetry)†	As-O Stretching Vibrations(cm^{-1}) ‡			
	As-OX (X = H^+, cation)		As-O (uncomplexed)	
	ν_{as}	ν_s	ν_{as}	ν_s
$Na_3AsO_4{\cdot}12H_2O$ ($C_3 \rightarrow Td$) As-O = 1.67 Å (4)	818_R (ν_s)[a], 786_R (ν_{as})[a]			
$Na_2HAsO_4{\cdot}7H_2O$ (C_1)	ν_s: 711_{IR}(shoulder at 756)[b]		885_{IR}[b]	825_{IR}[b]
As-OH = 1.74 Å As-O = 1.66, 1.67, 1.68 Å	737_R[a]		852_R[a]	835_R[a]
$NaH_2AsO_4{\cdot}2H_2O$ (C_{2v})[a]	770_R	788_R	912_R	804_R (H-bond)
KH_2AsO_4 (S_4)	792_R[a], all As-O bonds are equal & form 4 H-bonds			
High temperature form[c]	ν: 745-735		ν: 870-860	
$NH_4H_2AsO_4$[c]	ν: 750-730		ν: 870-850	
betaine H_2AsO_4[d]	791_R, 780_{IR}	727_R, 725_{IR}	913_R, 928_{IR}	874_R, 881_{IR}
betaine H_3AsO_4[d]	808_R, 833_{IR} (E)	791_R, 780_{IR}	ν_s: 970_R	
$CaHAsO_4{\cdot}2H_2O$ (haidingerite)[b] (C_1) As-OH = 1.77 Å As-O = 1.67, 1.65 (2) Å	As-OH ν_s: 737_{IR} (shoulder at 722), 724_R As-OCa&/H_2O ν_s: $871_{IR,R}$; ν_{as}: $894_{IR,R}$ unassigned: $800_{IR,R}$, $833_{IR,R}$ (impurities)			
$CaHAsO_4{\cdot}2H_2O$ (pharmacolite)[b] (C_1) As-OH = 1.73 Å As-O = 1.66, 1.68 (2) Å	As-OH ν_s: 737_{IR} (shoulder at 722), 726_R As-OCa/H_2O ν_s: $871_{IR,R}$; ν_{as}: $899_{IR,R}$ unassigned: $800_{IR,R}$, $833_{IR,R}$ (impurities)			
$Ca_5(HAsO_4)_2(AsO_4)_2{\cdot}4H_2O$ (sainfeldite)[b] (C_1) As1-OH = 1.73 Å As1-O = 1.66, 1.68, 1.69 Å As2-O = 1.69 (4) Å	As1-OH ν_s: 713_{IR}, 719_R As1-OCa ν_s: $869_{IR,R}$, ν_{as}: $895_{IR,R}$ As2-OCa/H_2O ν_s: $824_{IR,R}$, ν_{as}: $852_{IR,R}$			
$(Ca,Na)_3(Mg,Mn)_2(AsO_4)_3$ berzelite[b]	770_R	780_R	902_R	846_R
$Fe_3(AsO_4)_2{\cdot}8H_2O$ (simplesite)[e]	ν_s: 780		ν_s: 850	
$FeAsO_4{\cdot}8H_2O$ (scorodite)[b]	813_R	806_R	833	893_R
poorly crystalline Al-arsenate[g]	ν_s: 740_{IR}		ν_{s+} ν_{as}: 887_{IR}	
$Co_3(AsO_4)_2{\cdot}8H_2O$ (erythrite)[b]	ν_s: 794_R		ν_{s+} ν_{as}: 853_R	
$Co(NH_3)_5(AsO_4){\cdot}5H_2O$[f]	ν_s: 800_{IR}		851_{IR}	817_{IR}
$Co(NH_3)_4(AsO_4){\cdot}5H_2O$[f]	ν_s: 769_{IR} (unassigned peak at ~ 720)		856_{IR}	
$Ni_3(AsO_4)_2{\cdot}8H_2O$ (annabergite)[b]	792_{IR}	804_R	843_R	859_R
$Cu_2(AsO_4)(OH){\cdot}8H_2O$ (olivenite)[e]	828_{IR}	790_{IR}	938_{IR}	860_{IR}
$Zn_3(AsO_4)_2{\cdot}8H_2O$ (koettigite)[e]	828_{IR}	790_{IR}	$890,868_{IR}$	845_{IR}

Subscripts R, and IR indicate that the data is collected using Raman and IR spectrometers. Superscripts represent the references. a) Vasant et al. (1973), b) This study, c) Murphy et al. (1954), d) Haresh et al. (1995), e) Moenke (1962), f) Beech and Lincoln (1971), g) sample from B. Rochette and S. Fendorf, (University of Idaho). As1 and As2 represent two types of arsenate polyhedra.

† Site symmetry of the known minerals is shown in bold and in parenthesis.

‡ The symbol ν without any subscript represents unassigned As-O, or As-OX stretching vibrations.

metal atom, these are also modified by the type of metal-arsenate complex (number of coordinating metal atoms and their distance from As), and the intensity of H-bonding between H_2O and AsO_4^{3-} (e.g., As-OFe ν_s in scorodite and symplesite, Table 4). Unfortunately structural information on several solid metal arsenates and stability constants of their aqueous complexes are not available for comparison. Collectively, shifts in ν_s vibrations are small for several metal complexes as compared to the protonated AsO_4^{3-} (Table 3). Since these shifts are also similar to that of uncomplexed aqueous AsO_4^{3-} (excepting), the average As-O bond distance in these metal arsenates (especially for those of Ca, Fe, and Ni) and the uncomplexed AsO_4^{3-} ought to be very similar. X-ray diffraction and X-ray absorption spectroscopic studies support this hypothesis (Ferraris and Abbona, 1972; Kitahama et al., 1975; Myneni, 1995). With the exception of metal complexes of protonated and Al-AsO_4^{3-}, the ν_s of As-OM shifts to 780–810 cm^{-1} for different metal arsenate complexes (Table 4). The strongest interactions (with the smallest ν_s for As-OM) are noticed for complexes with softer cations, such as Pb^{2+} and Ba^{2+} (Baes and Mesmer, 1976; Moenke, 1966). Chemical shifts similar to those reported here are expected for As-OX ν_s vibrations when AsO_4^{3-} forms inner-sphere complexes on substrate surfaces.

Metal complexation with protonated arsenate. The spectral features of metal arsenates change completely when AsO_4^{3-} ions are protonated. In this case, the ν_s vibrations of As-OM

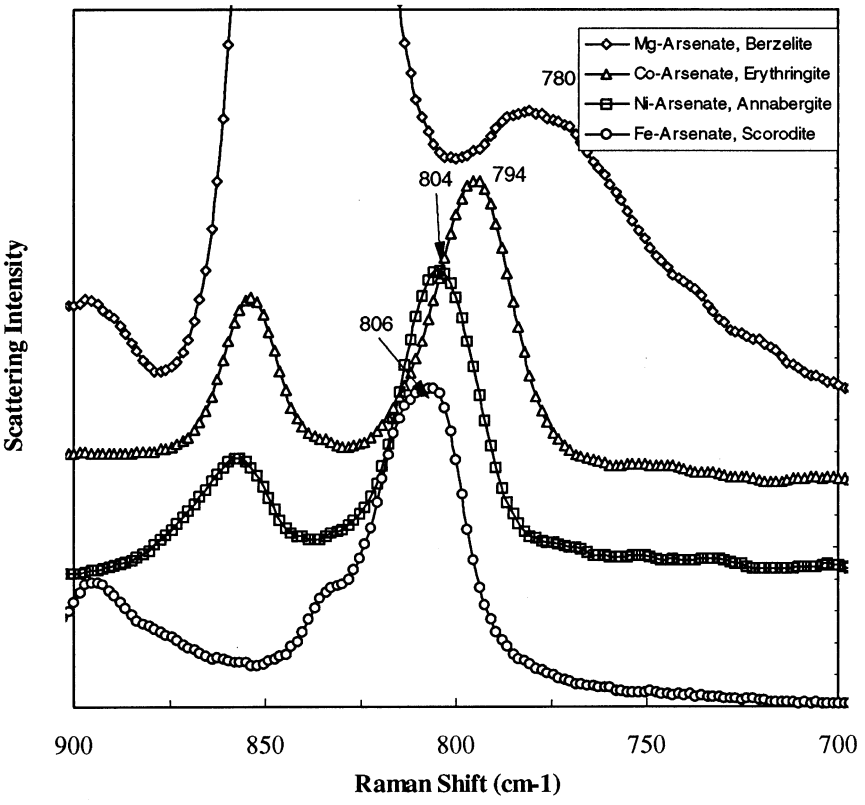

Fig. 6. Raman spectra of As-O stretching vibrations in crystalline metal arsenate salts. For spectral information see Table 4.

bonds do not follow the frequency range and trends discussed previously. In Fig. 7 and Table 4, the vibrational spectra, band assignments and As-O bond distances of protonated AsO_4^{3-} in different crystalline calcium arsenates, pharmacolite ($CaHAsO_4 \cdot 2H_2O$), haidingerite ($CaHAsO_4 \cdot 2H_2O$), and sainfeldite ($Ca_5(HAsO_4)_2(AsO_4)_2 \cdot 4H_2O$) are compared. In all of these complexes, $HAsO_4^{2-}$ complexes with Ca atoms and also forms H-bonds with H_2O molecules. However, the protonated O of $HAsO_4^{2-}$ does not complex with Ca and has an As-OH bond length of 1.73 ($\pm$0.01) Å. All other As-O distances (bonded to Ca and/or form H-bonds with H_2O) are in the range of 1.65–1.69 Å. When compared to the aqueous $HAsO_4^{2-}$ and uncomplexed $HAsO_4^{2-}$ of crystalline $Na_2(HAsO_4) \cdot 7H_2O$, the As-O bond distances in these calcium arsenates do not change with Ca complexation. Consequently the ν_s vibrations of As-OCa in these calcium arsenates and As-$O_{uncomplexed}$ in $HAsO_4^{2-}$ absorb IR radiation at similar wavenumbers (~866 cm^{-1}, Table 4). These features do not change when more than one Ca atom/H-bond links to $HAsO_4^{2-}$. This indicates that Ca complexation with the protonated arsenate does not substantially modify the symmetry of $HAsO_4^{2-}$. Similar spectral features were reported for several other protonated arsenate salts, and some of these are listed in Table 4.

Sainfeldite ($Ca_5(HAsO_4)_2(AsO_4)_2 \cdot 4H_2O$) has both protonated and unprotonated AsO_4^{3-} species, and its vibrational spectra exhibits two types of As-OX vibrations, where X = H^+, Ca, or H_2O (Table 4; Fig. 7). The relatively weak interactions of Ca and H_2O with unprotonated AsO_4^{3-} are apparent from the smaller shifts of its ν_s As-OCa (824 cm^{-1}). The As-O bond distances and the ν_s vibrations for these do not vary significantly from that of the uncomplexed, aqueous AsO_4^{3-} (818 cm^{-1}, Table 4). These features are significant when the spectra of mineral adsorbed AsO_4^{3-} are evaluated.

Outer-sphere metal-arsenate interactions. In arsenate salts such as $Na_3(AsO_4) \cdot 12H_2O$ and $Na_2(HAsO_4) \cdot 7H_2O$, AsO_4^{3-} forms extensive H-bonding with H_2O molecules of the Na octahedra, without any direct interactions with Na atoms. The site symmetries of AsO_4^{3-} in these salts are C_3 and C_1, respectively (Table 4). The As-O bond lengths are uniform with 1.67 Å in $Na_3(AsO_4) \cdot 12H_2O$ and hence its vibrational spectra exhibit features similar to those of tetrahedral AsO_4^{3-} (Tillmans and Baur, 1971; Vasant et al., 1973). In $Na_2(HAsO_4) \cdot 7H_2O$, the As-OH bond length is 1.74 Å, and the other three As-O bond lengths are 1.66, 1.67, and 1.68 Å (Table 4, Ferraris and Chiari, 1970). These differences in As-O bond distances are very small, and the H-bonded As-O cluster would probably display spectral splitting appropriate for C_{3v} symmetry due to insufficient spectral resolution. Accordingly, the As-O vibrations of $Na_2(HAsO_4) \cdot 7H_2O$ are similar to those of aqueous $HAsO_4^{2-}$. In both of these solids, H-bonding did not influence the As-O vibrations significantly, and their spectra exhibit features similar to those of respective ions in aqueous solutions. These two solids ought to be analogous to the AsO_4^{3-} outer-sphere complexes on mineral surfaces.

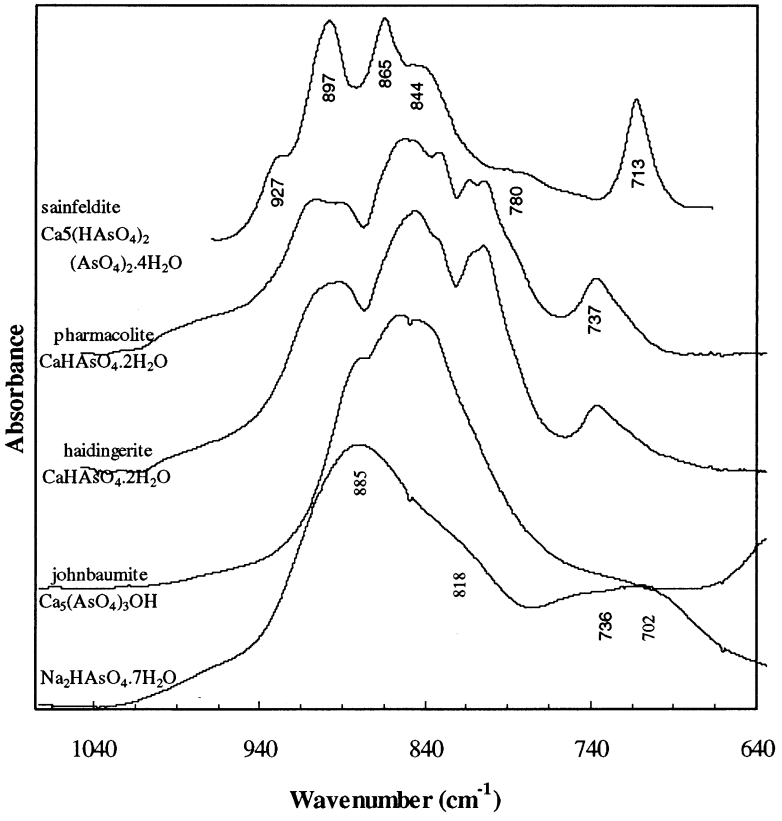

Fig. 7. Diffuse reflectance FTIR spectra of As-O vibrations in crystalline calcium AsO_4^{3-} salts.

3.2.4. Structure of AsO_4^{3-} adsorbed on mineral surfaces

Arsenate complexes on mineral surfaces can have different symmetries and the trends identified for As-O vibrations in protonated, solvated, and metal complexed arsenates are useful to predict their coordination chemistry. When AsO_4^{3-} sorbs on to mineral surfaces it may form outer- or inner-sphere complexes with the cation polyhedra and/or form a metal arsenate precipitate. Also the adsorption of AsO_4^{3-} and its protonated forms may take place simultaneously. In the following discussion, several examples of AsO_4^{3-} adsorption onto different substrate surfaces are presented.

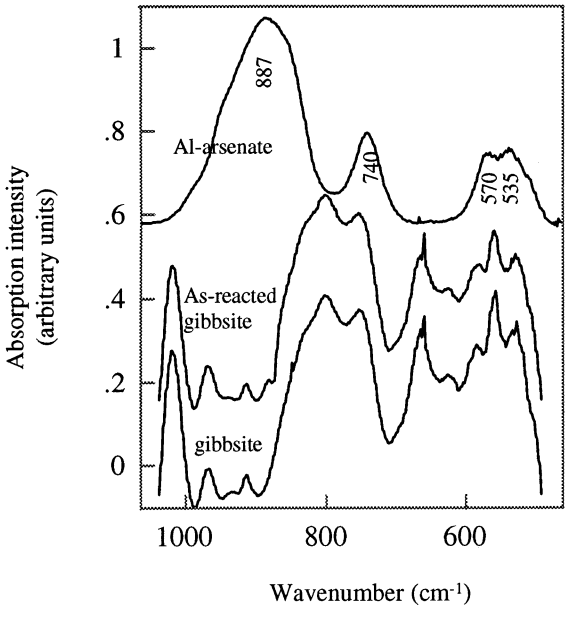

Fig. 8. Diffuse reflectance FTIR spectra of As-O vibrations in Al-arsenate and arsenate reacted gibbsite.

AsO_4^{3-} on Ca(OH)$_2$. The diffuse reflectance FTIR spectra of arsenate sorbed onto $Ca(OH)_2$ (pH = 12.7) exhibits peaks at 798–812, 879, and 885–905 cm^{-1} (Table 5). These peaks overlap each other with little splitting. Based on the number of bands, C_{3v} symmetry (corner-sharing with Ca polyhedra) can be assigned for the sorbed AsO_4^{3-}. However, similar weakly split vibrations can also be produced when AsO_4^{3-} forms more than one type of complex (edge and corner sharing), polydentate complexes (as in arsenate salts), and H-bonds with the surface Ca-OH functional groups. While the development of new OH bands at 3000 cm^{-1} support the formation of H-bonds between sorbed AsO_4^{3-} and structural OH, other suggested mechanisms can not be ruled out. Based on these observations and the trends described above, the bands at 798–812, 879, and 885–905 cm^{-1} are assigned to ν_s of As-OCa and ν_s and ν_{as} vibrations of $As\text{-}O_{uncomplexed}$, respectively. The absence of As-OH bands below 760 cm^{-1} and the presence of ν_s of As-OCa around 812 cm^{-1} in the sample DR-FTIR spectra indicate that the adsorbed AsO_4^{3-} is not protonated. The predominant aqueous arsenate species at these pH values is

Table 5. **As-O vibrations of AsO_4^{3-} adsorbed on mineral surfaces.**

Substrate	As-O Stretching Vibrations(cm^{-1})			
	As-OX (X = H^+, cation)		As-O (uncomplexed)	
	ν_{as}	ν_s	ν_{as}	ν_s
$Ca(OH)_2$[a]	ν_s: 798-812_{IR}		885-905_{IR}	879_{IR}
gibbsite[a]	Not clear, several overlapped Peaks		880 (identification not feasible)	
freshly prepared hydrous Fe-oxides[b]	As1-OH ν_s: 700_{IR} As2-OFe ν_s: 805_{IR}		As1-O : 875_{IR} (tentatively identified as ν_{as} As1-O/As-OFe)	
α-FeOOH (goethite)[c]	As1-OH ν_s: 730, 719_{IR} As2-OFe ν_s ~ 810_{IR}		As1-OFe/H-bonded ν_{as}: 834_{IR} As1-OFe/H-bonded ν_s: 938_{IR}	
Ag surface[d]	ν_S: 792_{SERS}		865_{SERS}	802_{SERS}

Subscripts IR and SERS indicate that the data is collected using IR and surface enhanced Raman spectrometers. Superscripts represent the references: a) This study, b) Harrison and Berkheiser (1982), c) Lumsdon et al. (1984), d) Haresh et al. (1995). As1 and As2 represent two types of arsenate polyhedra.

AsO_4^{3-}, which adsorbs on to $Ca(OH)_2$ surfaces without further modifications. Because of weak splitting in As-O vibrations, specific symmetry for adsorbed AsO_4^{3-} can not be assigned on the basis of available spectroscopic information.

AsO_4^{3-} on Al-hydroxides. Theoretical studies indicated that Al- should strongly distort arsenate tetrahedron and the As-O_{Al} vibrations should shift to very low wavenumbers when compared to the uncomplexed arsenate. The FTIR spectra of arsenate in poorly crystalline aluminum arsenate are in support of this and showed that the As-O_{Al} vibrations shifted to 740 cm^{-1}, with the As-$O_{uncomplexed}$ exhibiting a broad band at 887 cm^{-1} (Fig. 8). These broad bands represent the symmetric and asymmetric stretching vibrations of As-O_{Al} and As-$O_{uncomplexed}$, and their components can not be separated. Since the structure of this phase is not analyzed yet, the presence of traces of protonated arsenate in this sample may not be ruled out. Vibrational spectroscopic studies on well crystalline Al-arsenate phases are required to conclude the influence of Al bonding on arsenate vibrations.

The vibrational spectra of arsenate overlap with the vibrational spectra of gibbsite, which exhibits several broad peaks in the region of interest (1200–600 cm^{-1}, Fig. 8). However, the As-reacted gibbsite exhibits a small peak at 880 cm^{-1}, which is absent in the unreacted gibbsite spectrum. This peak also matches with the vibrations of As-$O_{uncomplexed}$ in poorly crystalline Al-arsenate previously described and may represent As-$O_{uncomplexed}$ vibrations of arsenate adsorbed on gibbsite. This may indicate that arsenate may directly bind to Al-polyhedra. However, As-O_{Al} vibrations could not be examined because of overlapping bands. The EXAFS analysis of arsenate-reacted gibbsite samples are also in support of the vibrational spectra and indicate that more than two Al atoms are complexed with arsenate polyhedra (Myneni, 1995).

AsO_4^{3-} on Fe-oxyhydroxides. Arsenate adsorption on freshly prepared hydrous iron oxides (Harrison and Berkheiser, 1982) and goethite (γ-FeOOH, Lumsdon et al., 1984) were reported previously. Their vibrational spectra band assignments are reinterpreted with the help of the trends discussed above for metal arsenates (Table 4). Arsenate reactions with freshly prepared hydrous iron oxide produced peaks at 700, 802, and 875 cm^{-1} (Table 5). A weakly IR absorption band at 700 cm^{-1} relates to the ν_s vibrations of As-OH in $HAsO_4^{2-}$. The corresponding As-$O_{uncomplexed}$ or As-OFe band is at 875 cm^{-1}. The weak band at 802 cm^{-1} may relate to the As-OFe ν_s vibrations of another unprotonated AsO_4^{3-}. Since the position of this band is too low for metal complexed $HAsO_4^{2-}$, this should represent another AsO_4^{3-} polyhedra complexed with Fe (compare Ca-arsenates discussed above). No more structural information can be derived from the available sample spectra. However, Harrison and Berkheiser (1982) reported a C_{2v} symmetry for adsorbed AsO_4^{3-} based on the appearance of three bands. As discussed earlier, these three bands actually should represent two structurally different arsenate complexes.

The IR spectra of AsO_4^{3-} adsorbed on goethite show peaks at 719, 730, 834, 938, and 1016 cm^{-1} (Lumsdon et al., 1984). While the bands at ~730 cm^{-1} are produced by As-OH ν_s vibrations (as in $HAsO_4^{2-}$), the bands at 834 and 938 cm^{-1} represent the corresponding ν_s and ν_{as} vibrations of As-OFe bonds, respectively. These spectra clearly indicate the adsorption of $HAsO_4^{2-}$ and this interpretation is in agreement with the interpretation of Lumsdon et al., 1984. However, their spectra also exhibit a distinct shoulder at the low energy side of the 834 cm^{-1} band, which may be around ~810 cm^{-1}. Lumsdon et al. (1994) did not report this band. As discussed in the above paragraph, this band may represent the ν_s vibrations of As-OFe and indicate the presence of another type of AsO_4^{3-} species. Since this As-OFe band exhibits very little shift for ν_s vibrations, the As-$O_{uncomplexed}$ of the same arsenate polyhedra may not deviate from that of aqueous AsO_4^{3-} and produce peaks in the vicinity of the broad peak around 834 cm^{-1}. These distinct sets of ν_s vibrations show the existence of both $HAsO_4^{2-}$ and AsO_4^{3-} on goethite surfaces. The nature of their complexation schemes are difficult to evaluate with the available IR spectra information. Two types of arsenate, bidentate binuclear and corner sharing complexes are identified from the EXAFS spectroscopic studies of arsenate sorbed onto goethite (Waychunas et al., 1993; Waychunas et al., 1995; Fendorf et al., 1997; Foster et al., 1998). While these studies do not distinguish the sorption of protonated and unprotonated arsenate, complete symmetry information can be obtained by combining the IR and EXAFS information. A recent IR study on arsenate sorbed onto goethite used the changes in OH (or OD in deuterated

samples) vibrations, such as peak intensity changes to predict arsenate geometry to be bidentate binuclear or tridentate (Sun and Doner, 1997). As discussed above, the mineral surface OH vibrations are modified by H-bonding and their spectra can produce the same features as if the surface OH are displaced. Hence arsenate geometry assignments solely on OH vibrational changes may be doubtful.

AsO_4^{3-} on Ag surface. With the help of surface enhanced Raman spectroscopy (SERS), Haresh et al. (1995) examined the sorption of $HAsO_4^{2-}$ on the Ag surface (Table 5). The spectra shows three distinct bands at 792, 802, and 865 cm^{-1}. These bands correspond to the ν_s of As-O_{Ag} and ν_s and ν_{as} of As-$O_{uncomplexed}$ vibrations. The appearance of these bands and their band shifts indicate that unprotonated AsO_4^{3-} binds weakly to the Ag surface as a monodentate corner-sharing complex. Absence of As-OH bands around 730 cm^{-1} rule out direct adsorption of $HAsO_4^{2-}$ which deprotonates before binding to the Ag surfaces. Similar bonding arrangement from SERS spectra have been reported by Greaves and Griffith (1988) for AsO_4^{3-} adsorption on Ag colloids. In this case study, the structure of the surface complex could be assigned more accurately because of the absence of protonated arsenate and clear splitting in the As-O vibrations.

In summary these studies on arsenate adsorbed on mineral/metal surfaces indicate that the AsO_4^{3-} coordination is difficult to identify when it is protonated. However, using both IR and Raman, the coordination of AsO_4^{3-} on substrate surfaces can be interpreted accurately when it is not protonated. These studies demonstrate that it is necessary to evaluate the nature of the sorption complex and its vibrational spectra in aqueous solutions before its coordination at the mineral-water interfaces is evaluated.

4. CONCLUSIONS

The IR and Raman spectra of aqueous and crystalline arsenates indicate that the AsO_4^{3-} geometry is strongly distorted by protonation, and the relative effects on AsO_4^{3-} polyhedra decrease in the order $H^+ \gg$ cation $\geq H_2O$. This trend is valid for several metal arsenates since none of the examined metals could produce strong shifts for As-O vibrations. In addition, metal complexation of protonated arsenate do not significantly change the group frequencies of that arsenate polyhedra. Protonation shifts As-OH ν_s band to wavenumbers <720, <770, and <790 cm^{-1} for $HAsO_4^{2-}$, $H_2AsO_4^-$, and $H_3AsO_4^0$, respectively. Metal complexation of a protonated arsenate does not change the As-O vibrations significantly from those of uncomplexed molecule. The shifts in corresponding As-$O_{uncomplexed}$ vibrations are also apparent at high wavenumbers. For the same type of complex, the shifts in ν_s band of As-OX vibrations (X = metal, H^+, H-bond to H_2O) relate to the bond strengths and are useful to predict the geometry of complexing species. Water H-bonding to AsO_4^{3-} produces changes in its OH vibrations, which are useful in the evaluation of H_2O coordination in the sorption complex.

Application of these trends in As-O vibrations to the evaluation of mineral sorbed arsenate should be approached with caution. During spectral interpretation, it is essential to make a distinction between the sorption of protonated versus unprotonated species. This has to be established before different types of arsenates and their coordination are evaluated. For the sorption of unprotonated arsenate complexes, the splitting in degenerate vibrations directly relates to the geometry of the sorbed arsenate complex. However, such features in the case of a sorbed protonated arsenate complex may not give significant information to determine its geometry. In such cases, combination of Raman and IR spectroscopic information can provide more structural information than each individual technique alone. Results similar to those presented here are also expected in the case of other oxoanion systems, and the trends described for arsenate can be applied to predict the bonding mechanisms for other tetrahedral oxoanions.

Acknowledgments—The authors would like to thank P. Chen and Prof. Mc Creery (Ohio State University) for helping in Raman data collection and providing the facilities, Prof. P. K. Dutta (Ohio State University) for discussions and helpful comments on the interpretation of vibrational spectra, P. Powhat, (Smithsonian Museums) and R. Tettenhorst (Ohio State University) for providing rare arsenate minerals, and B. Rochette and S. Fendorf (University of Idaho) for providing their synthetic Al-arsenate solid. The authors would also like to thank Prof. G. Sposito and T. Richardson (Lawrence Berkeley Laboratory) and the three anonymous reviewers for providing very useful comments. The research is supported by a grant program from the USGS-Water Resources Program. The principal author was supported by funding from DOE during the preparation of the manuscript (LBNL/LDRD). Additional salary and research support was provided by the Ohio Coal Development Office, The Ohio State University, and the Ohio Agricultural Research and Development Center (OARDC).

REFERENCES

Barger J. R., Towle S. N., Brown Jr., G. E., and Parks G. A. (1997) XAFS and bondvalence determination of the structures and compositions of the surface functional groups and Pb(II) and Co(II) sorption products on single-crystal (α-Al_2O_3). *J. Colloid Interface Sci*. **185,** 473–492.

Baur W. H. and Khan A. A. (1970) On the crystal chemistry of salt hydrates. VI. The crystal structures of disodium hydrogen orthoarsenate heptahydrate and of disodium hydrogen orthophosphate heptahydrate. *Acta Cryst.* **B 26,** 1584–1596.

Beech T. A. and Lincoln S. F. (1971) Arsenato Complexes of Cobalt (III). *Aust. J. Chem*. **24,** 1065–1070.

Bergström P., Lindgren J., Kristiansson O. (1991) An IR study of ClO_4^-, NO_3^-, I^-, Br^-, Cl^-, and SO_4^{2-} anions in aqueous solution. *J. Phys. Chem*. **95,** 8575–8580.

Bhagavantam S. and Venkataraidu T. (1969) *Theory of Groups and Its Application to Physical Problems*. Academic Press.

Brooker M. H. (1986) Raman spectroscopic measurements of ion hydration. In *The Chemical Physics of Solvation*. Part B. (Ed. R. R. Dogonadze et al.), pp. 119–184.

Brooker M. H. and Tremaine P. R. (1992) Raman studies of hydration of hydroxy complexes and the effect on standard partial molar heat capacities. *Geochim. Cosmochim. Acta* **56,** 2573–2577.

Brookins D.G. (1988) *Eh-pH Diagrams for Geochemistry*. Springer-Verlag.

Brown I. D. and Altermatt D. (1985) Bond-valence parameters obtained from a systematic analysis of the inorganic crystal structure database. *Acta Cryst*. **B 41,** 244–247.

Carlson L., Bigham J. M., Myneni S. C. B., and Traina S. J. (1998) Retention of Arsenic by Schwertmannite Formed Under Natural and Laboratory Conditions. To be submitted for *Chem. Geol*.

Cherry J. A., Shaikh A. U., Tallman D. E., and Nicholson R. V. (1979) Arsenic species as an indicator of redox conditions in groundwater. *J. Hydrology* **43,** 373–392.

Cotton F. A. (1971) *Chemical Applications of Group Theory*. Wiley Eastern Ltd.

Cruickshank D. W. J. and Robinson E. A. (1966) Bonding in orthophosphates and orthosulfates. *Spectrochim. Acta* **22,** 555–563.

Cullen W. R. and Reimer K. J. (1989) Arsenic speciation in the environment. *Chem. Rev*. **89,** 713–764.

Dove P. and Rimstidt (1985) The solubility and stability of scorodite. *Amer. Mineral*. **70,** 838–844.

Eysel H. H. and Wagner R. (1993). Raman intensities of liquids: Absolute scattering activities and electro-optical parameters (EOPs) of arsenate and selenate ions in aqueous solutions. *Spectrochim. Acta* **49 A,** 503–507.

Farmer V. C. (1974) *The Infrared Spectra of Minerals*. Miner. Soc.

Fateley W. G., Mcdevitt N. T., and Bentley F. F.(1971) Infrared and Raman selection rules for lattice vibrations: The Correlation Method. *Appl. Spectr*. **25,** 155–173.

Ferraris G. (1969) The crystal structure of pharmacolite $CaHAsO_4 \cdot 2H_2O$. *Acta Cryst*. **B25,** 1544–1550.

Ferraris G. and Abbona F. (1972) The crystal structure of $Ca_5(HAsO_4)_2(AsO_4)_2 \cdot 4H_2O$ (sainfeldite). *Bull. Soc. fr. Mineral. Cristallogr* **95,** 33–41.

Ferraris G. and Chiari G. (1970) The crystal structure of $Na_2HAsO_4 \cdot 7H_2O$. *Acta Cryst*. **B26,** 1574–1583.

Ferraris G., Jones D. W., and Yerkess J. (1972) Neutron and X-ray refinement of the crystal structure of $CaHAsO_4 \cdot H_2O$ (haidingerite). *Acta Cryst*. **B28,** 209–214.

Fendorf S. E., Eick M. J., Grossl P., and Sparks D. L. (1997) Arsenate and chromate retention mechanisms on goethite: 1. Surface structures. *Environ. Sci. Tech*. **31,** 315–320.

Foster A. L., Brown Jr., G. E., Tingle, T. N., and Parks G. A. (1997) Quantitative arsenic speciation in mine tailings using X-ray absorption spectroscopy. *Amer. Mineral*. **83,** 553–568.

Gillette P. C., Lando J. B., and Koenig J. L. (1982) Band shape analysis of Fourier Transform infrared spectra. *Appl. Spectr*. **36,** 401–404.

Greaves S. J. and Griffith W. P. (1988) Surface-enhanced Raman scattering from silver colloids of vanadate, phosphate and arsenate. *J. Raman Spectrosc*. **19,** 503–507.

Haresh R., Philip D., and Aruldhas G. (1995) Infrared, Raman and SERS spectra of betaine arsenate. *Spectrosc. Lett*. **28,** 11–28.

Harrison J. B. and Berkheiser V. (1982) Anion interactions with freshly prepared hydrous iron oxides. *Clays Clay Minerals* **30,** 97–102.

Kitahama K., Kiriyama R., and Baba Y. (1975) Refinement of the crystal structure of scorodite. *Acta Cryst*. **B 31,** 322–324.

Krestov G. A. et al. (1994) *Ionic Solvation*. Ellis Horwood.

Lumsdon D. G., Fraser A. R., Russell J. D., and Livesey N. T. (1984) New Infrared band assignments for the arsenate ion adsorbed on synthetic goethite (α-FeOOH). *J. Soil Sci*. **35,** 381–386.

Maddoms W. F. (1980) The scope and limitations of curve fitting. *Appl. Spectr*. **34,** 245–267.

Magini M., Licheri G., Paschina G., Piccaluga G., and Pinna G. (1988) *X-ray Diffraction of Ions in Aqueous Solutions: Hydration and Complex Formation*. CRC Press.

Markham G. D.. Glusker J. P., Bock C. L., Trachtman M., and Bock C. W. (1996) Hydration energies of divalent beryllium and magnesium ions: An ab initio molecular orbital theory. *J. Phys. Chem*. **100,** 3488–3497.

Masscheleyn P. H., Delaune R. D., and Patrick W. H., Jr. (1991) Effect of redox potential and pH on arsenic speciation and solubility in a contaminated soil. *Environ. Sci. Tech*. **25,** 1414–1419.

Moenke H. (1962) *Mineralspektren* I. Akademie-Verlag.

Moodenbaugh A. R., Hartt J. B., and Hurst J.. (1983) Neutron Diffraction study of polycrystalline H_2SO_4 and H_2SeO_4. *Phys. Rev*. **B 28,** 3501–3505.

Mueller A. and Krebs B. (1967) Normal coordinate analysis of XY_4 tetrahedral molecules. *J. Mol. Spectrosc*. **24,** 180–198.

Murphy G. M., Weiner G., and Oberley J. J. (1954) IR reflection spectra of phosphate and arsenate crystals. *J. Chem. Phys*. **22,** 1322.

Myneni S. C. B. (1995) Oxyanion-Mineral Surface Interactions in Alkaline Environments: Arsenate and Chromate Sorption and Desorption in Ettringite. Ph. D Dissertation. Ohio State University.

Myneni S. C. B., Traina S. J., Logan T. J., and Waychunas G. A. (1997) Oxyanion behavior in alkaline environments: Sorption and desorption of arsenate in ettringite. *Environ. Sci. Tech*. **31,** 1761–1768.

Myneni S. C. B. Traina S. J., Waychunas G. A., and Logan T. J. (1998) Vibrational spectroscopy of functional group chemistry and arsenate coordination in ettringite. Next issue of *Geochim. Cosmochim. Acta*.

Nakamoto K. (1986) *Infrared and Raman Spectra of Inorganic and Coordination Compounds*. Wiley.

Nakamoto K., Margoshes M., and Rundle R. E. (1955) Stretching frequencies as a function of distances in hydrogen bonds. *J. Amer. Chem. Soc*. **77,** 6480–6486.

Ouafik Z., Le Calvé N., and Pasquier B. (1995) Vibrational study of various crystalline phases of thallium dihydrogen arsenate TlH_2AsO_4. Comparison with thallium dihydrogen phosphate TlH_2PO_4. *Chem. Phys*. **194,** 145–158.

Ouafik Z. Brulé D., Pasquier B., and Le Calvé N (1996) Vibrational study of the disordered paraelastic high-temperature phase of thallium dihydrogen arsenate, TlH_2AsO_4. *J. Raman Spectrosc*. **27,** 1–8.

Ohtaki H. and Radnai T. (1993) Structure and dynamics of hydrated ions. *Chem. Rev*. **93,** 1157–1204.

Persson P., Nilsson N., and Sjoberg S. (1996). Structure and bonding of orthophosphate ions at the iron oxide-aqueous interface. *J. Colloid Intl. Sci*. **177,** 263–275.

Pokrovski G., Gout R., Schott J., Zotov A., and Harrichoury J. -C. (1996) Thermodynamic properties and stoichiometry of As(III) hydroxide complexes at hydrothermal conditions. *Geochim. Cosmochim. Acta* **60,** 737–749.

Payen E., Grimblot J., and Kasztelan S. (1987) Study of oxic and reduced alumina-supported molybdate and heptamolybdate species by in-situ laser Raman spectroscopy. *J. Phys. Chem*. **91,** 6642–6648.

Ross S. D. (1974) Phosphates and other oxy-anions of group V. In *The Infrared Spectra of Minerals* (ed. V. C. Farmer), pp. 383–422. Mineral.l Soc. London.

Seeger D. M., Korzeniewski C., and Kowalchyk W. (1991) Evaluation of vibrational force fields derived by using semiempirical and *ab initio* methods. *J. Phys. Chem*. **95,** 6871–6879.

Siebert H. (1954) Struktur der sauerstoffsäuren. *Z. Anorg. Allg. Chem*. **275,** 225–240.

Siebert H. (1966) *Anwendungen der schwingungsspektroskopie in der anorganischen chemie*. Springer-Verlag.

Soma M., Tanaka A., Seyama H., and Satake K. (1994). Characterization of arsenic in lake sediments by X-ray photoelectron spectroscopy. *Geochim. Cosmochim. Acta* **58,** 2743–2745.

Sposito G. (1989) *The Chemistry of Soils*. Oxford Univ. Press.

Stewart J . J. P. (1989a) Optimization of parameters for semiempirical methods: I. Method. *J. Comp. Chem*. **10,** 209–220.

Stewart J. J. P. (1989b) Optimization of parameters for semiempirical methods: II. Applications, *J. Comp. Chem*. **10,** 221–264.

Stumm W. (1993) *Chemistry of the Solid-Water Interface*, Wiley-Interscience Publ.

Sun X. and Doner H. E. (1996) An investigation of arsenate and arsenite bonding structures on goethite by FTIR. *Soil Sci*. **161,** 865–872.

Tillmans E. and Baur W. H. (1971) On the crystal chemistry of salt hydrates. VII. The crystal structures of pseudo trisodium ortho arsenate dodecahydrate and the isomorphous phosphate and vanadate salts. *Acta Cryst*. **B 27,** 2124-2139.

Tossell J. A. (1997) Theoretical studies on arsenic oxide and hydroxide species in minerals and in aqueous solution. *Geochim. Cosmochim. Acta* **61,** 1613–1623.

Twu J. and Dutta P. K. (1989) Structure and reactivity of oxovanadate anions in layered lithium aluminate materials. *J. Phys. Chem*. **93,** 7863–7868.

Vasant F. K., Van Der Veken B. J., and Desseyn H. O. (1973) Vibrational analysis of arsenic acid and its anions. I Description of the Raman spectra. *J. Mol. Struct*. **15,** 425–437.

Waychunas G. A., Rea B. A., Fuller C. C., and Davis J. A. (1993) Surface chemistry of ferrihydrite: Part 1. EXAFS studies of the geometry of coprecipitated and adsorbed arsenate. *Geochim. Cosmochim. Acta* **57,** 2251–2269.

Waychunas G. A., Rea B. A., Davis J. A., and Fuller C. C. (1995) Geometry of sorbed arsenate on ferrihydrite crystalline FeOOH: Reevaluation of EXAFS results and topological factors in predicting geometry and evidence for monodentate complexes. *Geochim. Cosmochim. Acta*. **59,** 3655–3661.